



Neuro-fuzzy Control of Laser Percussion Drilling

Martin M. Ruthandi*¹, Bernard W. Ikuu¹, George N. Nyakoe¹ and James N. Keraita²

¹Department of Mechatronic Engineering, Jomo Kenyatta University of Agriculture and Technology, Juja. P.O. Box 62,000-00200 Nairobi, Kenya.

²School of Engineering, Dedan Kimathi University of Technology, Nyeri. P.O Box 657- 10100 Nyeri, Kenya.

*Corresponding Author - Email: mmaina@jkuat.ac.ke

Abstract Non-Conventional methods have recently been employed in the drilling of materials such as super alloys which are hard to machine using mechanical conventional methods. These materials are mainly used in turbines in the power generation and aerospace industries. One of the recently developed non-conventional methods for drilling is using pulsed lasers whereby a laser beam is focussed to a spot equal in diameter to the hole to be drilled. Pulsed lasers such as Nd:YAG are mainly employed for this process. Laser percussion drilling is commonly employed to produce holes with small diameters, usually less than 1mm. With percussion drilling, the control of hole parameters such as taper, entrance and exit hole variation and roundness is difficult and these parameters are of utmost importance for small holes. Selection of machining parameter combinations for obtaining optimum circularity at entry and exit and minimum hole taper is a challenging task owing to the presence of a large number of process variables. There is therefore need to develop a control system that is able to adjust the various process parameters to the optimum values and hence control the drilling process. This paper discusses a neuro-fuzzy controller developed to control the hole diameters and taper through in-process adjustments of laser power and pulse duration. The controller is based on *MATLAB* and *LabVIEW* platforms. The controller was implemented by simulating a laser drilling environment. It is seen that while using the controller, the diameters increase with increase in peak power and pulse duration up to an optimum level beyond which the peak power and pulse duration do not increase. The hole taper decreases with increase in peak power and pulse duration up to optimum level beyond which the peak power and pulse duration do not increase. Thus, the controller helps maintain the peak power and pulse duration at optimum levels.

Keywords Hole taper, Laser Percussion drilling, Neuro-fuzzy control, Peak power, Pulse duration.

1. Introduction

It is difficult to produce macro or micro holes of high aspect ratio in super alloys using conventional machining processes [1]. High tool wear and excessive heat generation have rendered mechanical drilling unsuitable for such purposes [2], [3]. Past studies have shown that laser drilling is well suited for the drilling of thermal barrier coated (TBC) super-alloys since both the ceramic and metallic layers can be processed [1]–[5]. In comparison, the competing technology of electrical discharge machining is limited to conducting substrates and therefore cannot machine TBC coated components [4], [6]. An example of nickel based super alloys is Inconel 718. Such alloys have mainly been employed in steam turbines for power generation and jet engines [5], [7].

In laser percussion drilling, a series of short pulses (10^{-12} to 10^{-3} s) separated by longer time periods (10^{-2} s) are directed on the same spot to drill. Each laser pulse contributes to the drilling by removing a small volume of

material. Pulsed Nd:YAG lasers are most commonly used for percussion drilling because of their higher energy per pulse. Percussion drilling is used to produce holes of upto 1.3 mm diameter on metal plates of upto 25 mm thick [8], [9].

The high machining rate of laser percussion drilling makes the drilling method a prime candidate for drilling such components as combustion chambers, which have between 40,000 to 50,000 holes. Other components such as turbine and guide vanes contain fewer holes, typically 50 to 200, but given the total number of components involved, percussion drilling still has the potential to provide significant cost-benefit [10].

The determination of efficient laser process parameters and laser beam parameters for the drilling process is a major challenge for the power generation and aerospace industry [11], [12]. Therefore there is need to control the laser percussion drilling process in order to avoid the imperfections such as tapering and non-circularity which



have adverse effects on the airflow over the surface of the component affecting the lifespan of the component [13], [14].

2. Neuro-Fuzzy Learning and Control Approach

Neuro-fuzzy systems represent a newly developed class of hybrid intelligent systems combining the main features of artificial neural networks with those of fuzzy logic systems [15], [16]. The main aim of combining neural networks and fuzzy logic is to circumvent difficulties encountered in applying fuzzy logic for systems represented by numerical knowledge (data sets), or conversely in applying neural networks for systems represented by linguistic information (fuzzy sets). Neither fuzzy reasoning systems nor neural networks are by themselves capable of solving problems involving both linguistic and numerical knowledge [17], [18].

The integration of fuzzy logic systems with neural networks aids fuzzy systems in learning and strengthens the neural network features in terms of explicit knowledge representation.

Neuro-fuzzy systems (NFS) can be divided into three major categories, according to their topologies and functionalities [15], [19]. These are; Cooperative neuro-fuzzy systems, Neural network-driven fuzzy reasoning systems, and Hybrid neuro-fuzzy systems

Of interest in this study is the Hybrid neuro-fuzzy system. This is based on an architecture which integrates a neural network and a fuzzy logic-based system in an appropriate parallel structure. The fuzzy logic system and the neural network operate as one synchronized entity [17].

Hybrid neuro-fuzzy systems have a parallel architecture, and exploit similar learning paradigms, as is the case for neural networks. The parallelism of the system can be viewed as a mapping of the fuzzy system into a neural network structure. Each functional module of the fuzzy logic system corresponds to a particular layer of the neural network. The resulting system can be interpreted either as a neural network or a fuzzy logic system [19], [20]. Figure 1 depicts the mapping from a fuzzy logic system to a neural network structure.

The structure of the system can be described layer by layer as follows [17], [19]:

Layer 1: Fuzzification–This layer consists of a set of linguistic variables. The crisp inputs x_1 and x_2 are fuzzified through mapping into membership functions of the linguistic variables, which usually take triangular, trapezoid, or bell-shaped membership functions.

Layer 2: Rule nodes–This layer contains one node per each fuzzy if-then rule. Each rule node performs a connective operation within the rule antecedent (*if* part). Usually, the minimum or the dot product is used as the T-norm operator to represent the connective AND. The union OR connective is usually represented using the maximum operation or any other T-conorm operator.

Layer 3: Normalization–In this layer, the firing strengths

of the fuzzy rules are normalized. The normalized firing strength is given by;

$$\bar{w}_p = \frac{w_p}{\sum_{i=1} w_i} \tag{1}$$

where w_p is the firing strength of the p-th rule.

Layer 4: Consequent layer–This layer is related to the consequent of the fuzzy rule. The values of the consequent (*then* part) are multiplied by normalized firing strengths according to:

$$\bar{O}_p = \bar{w}_p O_p \tag{2}$$

where \bar{O}_p is the consequent layer output and O_p is the normalization layer output.

Layer 5: Summation–This layer computes the overall output as the summation of the incoming signals:

$$O^* = \sum_p \bar{O}_p \tag{3}$$

where O^* is the overall output.

A common example of a hybrid neuro-fuzzy system is the Adaptive-Neuro-Fuzzy Inference System (ANFIS), which can be represented in a four or five layer architecture [17], [21], [22].

3. Development of the Neuro-Fuzzy Controller

3.1. ANFIS Model

It is proposed to use Sugeno inference mechanism for the ANFIS due to its ability to model non-linear systems [19], [23]. In this type of inference mechanism, the output is a function of the inputs and is a fuzzy singleton. ANFIS involves three major steps namely: Identification of inputs, outputs and their ranges; Design of membership functions and rule base; and Mapping of fuzzy outputs to corresponding crisp values.

3.1.1. Identification of inputs, outputs and their ranges

The inputs to the ANFIS model are the taper angle and diameter at hole exit. The values of these inputs are derived from experimental work as reported by Joonghan Shin and Satapathy [24], [25]. Joonghan carried out Laser drilling of Inconel 718. The laser used was a high average power diode-pumped solid state Nd:YAG laser operated at 1064 nm. Drilling was carried out on Inconel 718 plates 3 mm thick, 5 mm wide, and 25 mm long. Satapathy carried out laser drilling on a medium carbon steel specimen, 100 mm long, 10 mm wide, and 8 mm thick. A pulsed Nd-YAG laser system was used with a rated average power of 100 W. The set of data obtained from these experiments was used to train and test the ANFIS for this work.

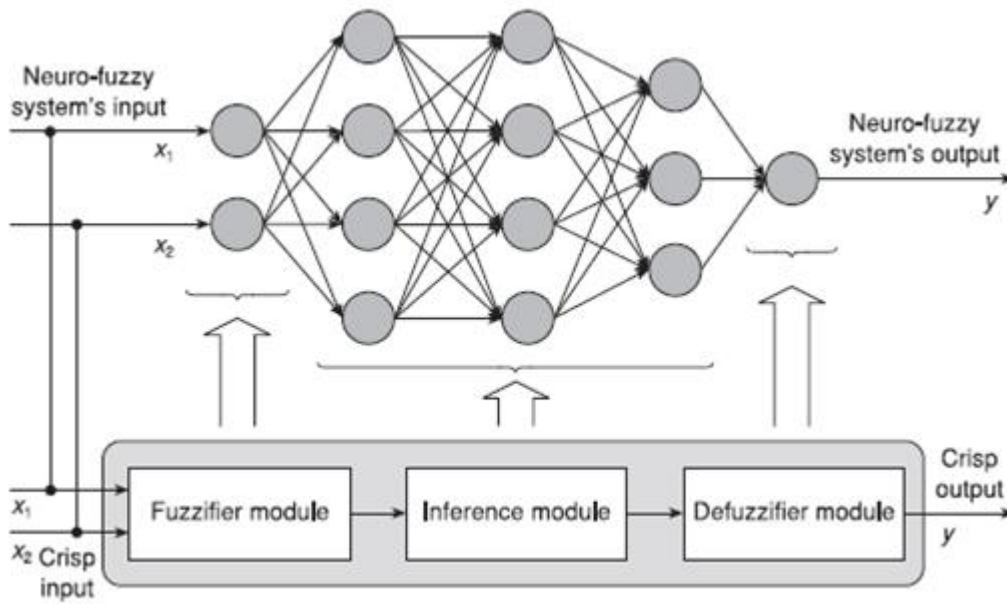


Fig. 1. Mapping from a fuzzy logic system to a neural network structure [19]

Figure 2 shows the block representations of ANFIS. The inputs into the ANFIS are diameters at the exit and hole taper angles. The outputs are laser peak power and pulse durations.

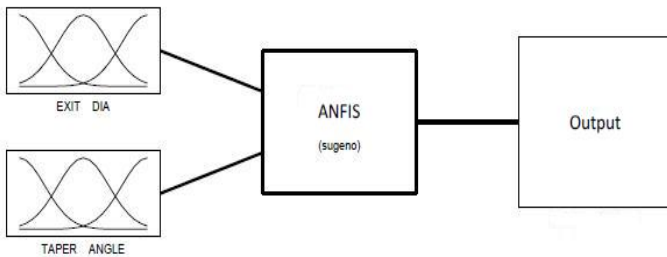


Fig. 2. Block representation of ANFIS

3.1.2. Design of membership functions and rule base

The design of membership functions was achieved as follows:

A set of training data, which constitutes the laser drilling conditions and the expected output, is presented to the ANFIS. The ANFIS is generated by use of grid partitioning, which is a method for grouping data into clusters based on their similarity. The ANFIS is then trained by use of hybrid learning rule. The hybrid learning rule combines the gradient method and the least squares estimate (LSE).

The ANFIS is then tested against a set of testing data. Different sets of data are presented to the ANFIS, and based on the input-output relationship of the ANFIS, the membership functions are constructed. The membership functions for the two inputs are similar but with different universe of discourse. The membership functions for the diameter at the exit are shown by Fig. 3.

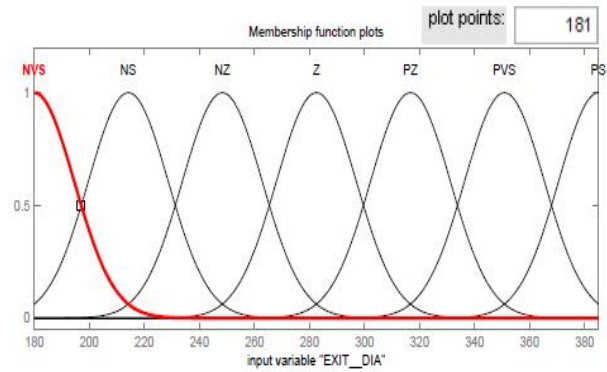


Fig. 3. Membership functions for hole diameter at the exit

Gaussian type membership functions are used for the two inputs because they represent the non-linear nature of the problem in a better way than triangular or trapezoidal membership functions. The membership function definition is as shown in Table 1.

Table 1. Membership functions definition

Symbol	Meaning
NVS	Negative very small
NS	Negative small
NZ	Negative zero
Z	Zero
PZ	Positive zero
PVS	Positive very small
PS	Positive small

The rule base for the fuzzy logic controller (FLC) is then generated based on the execution of the ANFIS. ANFIS automatically generates its own rule base depending on its set of training data.



3.1.3. Mapping of fuzzy outputs to corresponding crisp values

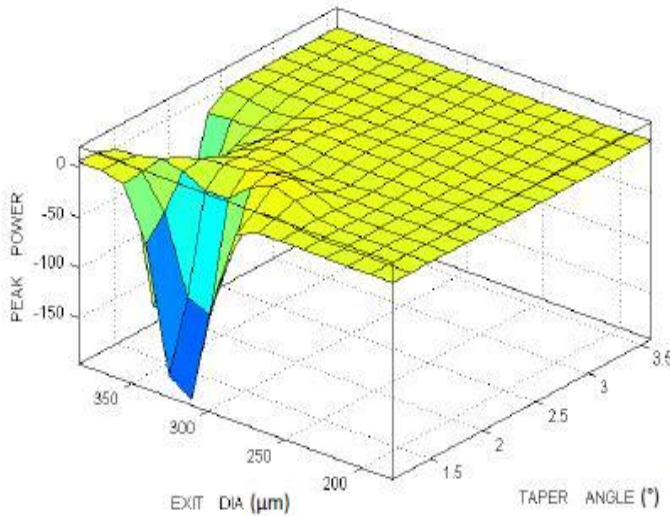


Fig. 4. Surface map for exit diameter and taper angle

The surface map generated by ANFIS for laser power is shown in Fig. 4. The surface map shows the mapping from diameter at the exit and hole taper to laser peak power. The surface map helps examine the output surface of a FIS stored in a file for any one or two inputs.

Fig. 5 shows a diagrammatic representation of some of the rules for the ANFIS. It shows the crisp output (laser power) of 3.22 kW with diameter at the exit being 283 μm and taper angle of 2.38°. There are a total of 49 rules. If one or both input values are changed, then the output changes as per the rules to give the optimum laser power.

The ANFIS was presented with different input sets so as to simulate a machining situation. The results were used in the design of the input and output membership functions as well as in the generation of the rules for the Fuzzy Logic Controller.

3.2. Design of the Fuzzy Logic Controller

LabVIEW software was used to develop the fuzzy logic controller. Fig. 6 shows a section of the controller while Fig 7 shows the front panel for the controller, displaying some controller outputs.

As can be seen in Fig. 6, implementation of the FLC involves referencing a fuzzy system designed on LabVIEW and saved as a .fs file, and reading of input data from a spreadsheet file. The input data includes values of hole diameters at the exit and taper angles derived from a laser drilling model. The controller computes values for the diameter at the hole entrance. Input values are recorded as the controller runs.

Fuzzy Logic control is then performed based on the information received on the shift register. The initial information comes from the .fs file. The output values are then computed based on the control action. The output

parameters are laser power and the pulse duration. These outputs values are recorded as the controller runs.

The controller checks if the control has a different value from the previous loop iteration. It then gets the membership functions points of the input and output variables and change the values using a simple shifting algorithm. Membership functions points are then set with updated values.

The effectiveness of the controller was tested by comparing the controller results with results from a laser drilling model. The model was developed using Finite Element Method and was based on COMSOL which is a Finite Element Analysis software package that allows the user to develop 3D models with associated boundary conditions. COMSOL was used for simulation purposes to mathematically model the laser drilling process. A fine mesh is used for the entire model. A Q-switched Nd:YAG laser was employed. With this type of laser, high laser power in the range of Kilowatts can be achieved. It is also possible to obtain modulated laser pulses in the range of milliseconds. An image analyzer, was used to analyze the images generated. The model was then validated using experimental data obtained from drilling of Stainless steel sheets as reported by Wei Han [13]. The conditions for the experimental work by Wei Han [13] is summarized in Table 2. Values of hole diameters and taper angles were measured and recorded. This data was used to validate the laser drilling model.

Table 2. Machining conditions for experimental work [13]

Machining condition	Description
Material	304 Stainless steel
Material thickness	2.4 mm
Laser equipment	Pulsed Nd:YAG laser
Laser wavelength	1.06 μm
Laser peak power	1.5-4 kW
Laser energy per pulse	1.75-4 J
Pulse frequency	1-10 Hz
Pulse width	0.5-2 ms
Lens focal length	100 mm
Beam spot size	80 μm

4. Results and Discussions

Two simulations were carried out using the laser drilling model. For the first simulation, the laser drilling model was simulated to test the effects of peak power on laser drilling of Nickel super alloy-Inconel 718. Peak power was varied from 1 kW to 6 kW. The model output showed minimum and maximum entrance hole diameters of 400 μm and 570 μm respectively, minimum and maximum exit hole diameters of 50 μm and 450 μm respectively, and minimum and maximum hole taper of 1.2° and 3.4° respectively.

For the second simulation, the laser drilling model was simulated to test the effects of varying laser pulse duration at a constant peak power of 3 kW. The pulse duration was varied from 1 ms to 6 ms. The model output showed minimum and maximum entrance hole diameters of 390 μm

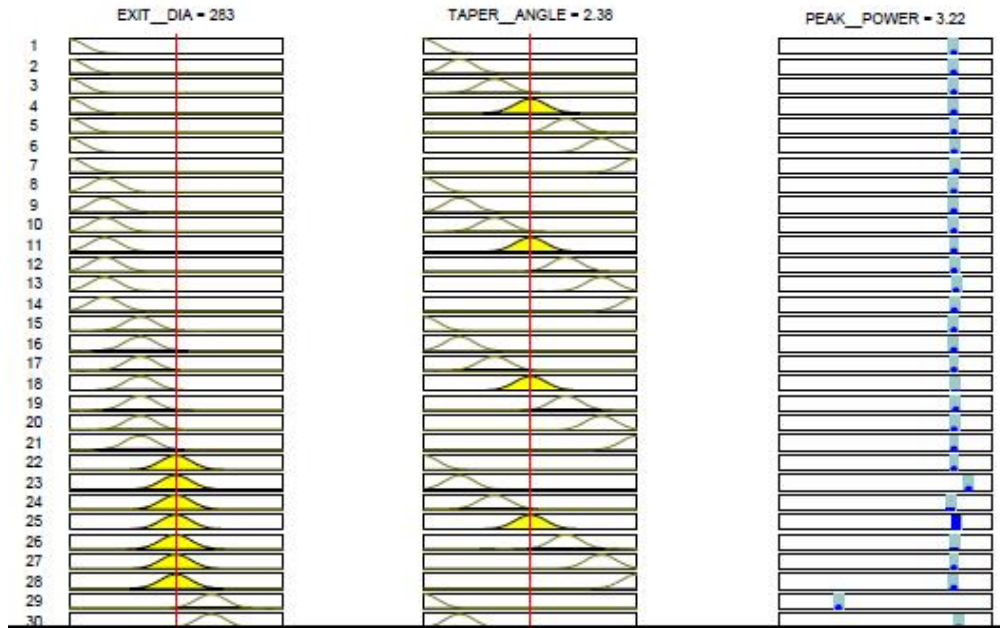


Fig. 5. Diagrammatic representation of some of the rules for the ANFIS

and $580\ \mu\text{m}$ respectively, minimum and maximum exit hole diameters of $70\ \mu\text{m}$ and $470\ \mu\text{m}$ respectively, and minimum and maximum hole taper of 1.4° and 3.6° respectively.

Output data from the model was used as the input to the controller. The controller simultaneously controlled laser peak power and pulse duration. Data from the first simulation was used and included values for taper angle and exit diameter while varying the peak power at fixed pulse duration of 2 ms. The results obtained from the controller are shown in following figures.

Fig. 8 shows the variation of hole diameters with laser peak power. The diameters are seen to generally increase as the power increases. This increase is to be expected since the laser beam intensity at a spot increases with increasing power. For exit hole diameters ranging from $50\ \mu\text{m}$ to $450\ \mu\text{m}$, the maximum laser peak power was found to be 2.082 kW.

The variation of hole taper with laser peak power is shown in Fig. 9. The taper is seen to generally reduce as the power increases. For hole taper angles ranging from 1.2° to 3.4° , the maximum laser peak power was found to be 2.082 kW.

Fig. 10 shows the variation of hole diameters with laser pulse duration. The diameters are seen to generally increase as the pulse duration increases. This increase is to be expected since the energy delivered at the spot increases with increasing pulse width. For exit hole diameters ranging from $50\ \mu\text{m}$ to $450\ \mu\text{m}$, the maximum laser pulse duration was found to be 1.669 ms.

The variation of hole taper with laser pulse duration is shown in Fig. 11. The taper is seen to generally reduce as the pulse duration increases. For hole taper angles ranging from 1.2° to 3.4° , the maximum laser pulse duration was found to be 1.669 ms.

From Figs 12 and 13, it can be deduced that while drilling using the neuro-fuzzy controller, the laser peak power and pulse duration can be simultaneously varied in order to acquire optimal hole parameters.

The controller results were compared with model input-output data. While drilling without the controller, the hole diameters increase with increasing laser peak power and pulse duration. Increasing laser peak power at a fixed pulse duration increases the laser beam intensity at the drilling spot.

Figures 14 and 15 show the rates of change of hole diameters and taper with increase in peak power at a constant pulse duration. The entrance and exit diameters increases at rates of 0.0336 mm/kW and 0.0814 mm/kW respectively. The hole taper decreases at a rate of 0.45 deg/kW.

Increasing the pulse width at fixed peak power effectively increases energy per pulse of the laser beam. This will generate high vapor pressure built up inside the hole and ejecting more material. Figures 16 and 17 show the rates of change of hole diameters and taper with increase in pulse duration at a constant peak power. The entrance and exit diameters increases at rates of 0.0334 mm/ms and 0.0809 mm/ms respectively. The hole taper decreases at a rate of 0.881 deg/ms.

While using the controller, the hole diameters increase with increase in peak power and pulse duration upto an optimum level beyond which the peak power and pulse duration remain constant as the diameters increase. The hole taper decreases with increase in peak power and pulse duration upto optimum level beyond which the peak power and pulse duration remain constant as the taper decreases. Thus, the controller helps maintain the peak power and pulse duration at optimum levels.

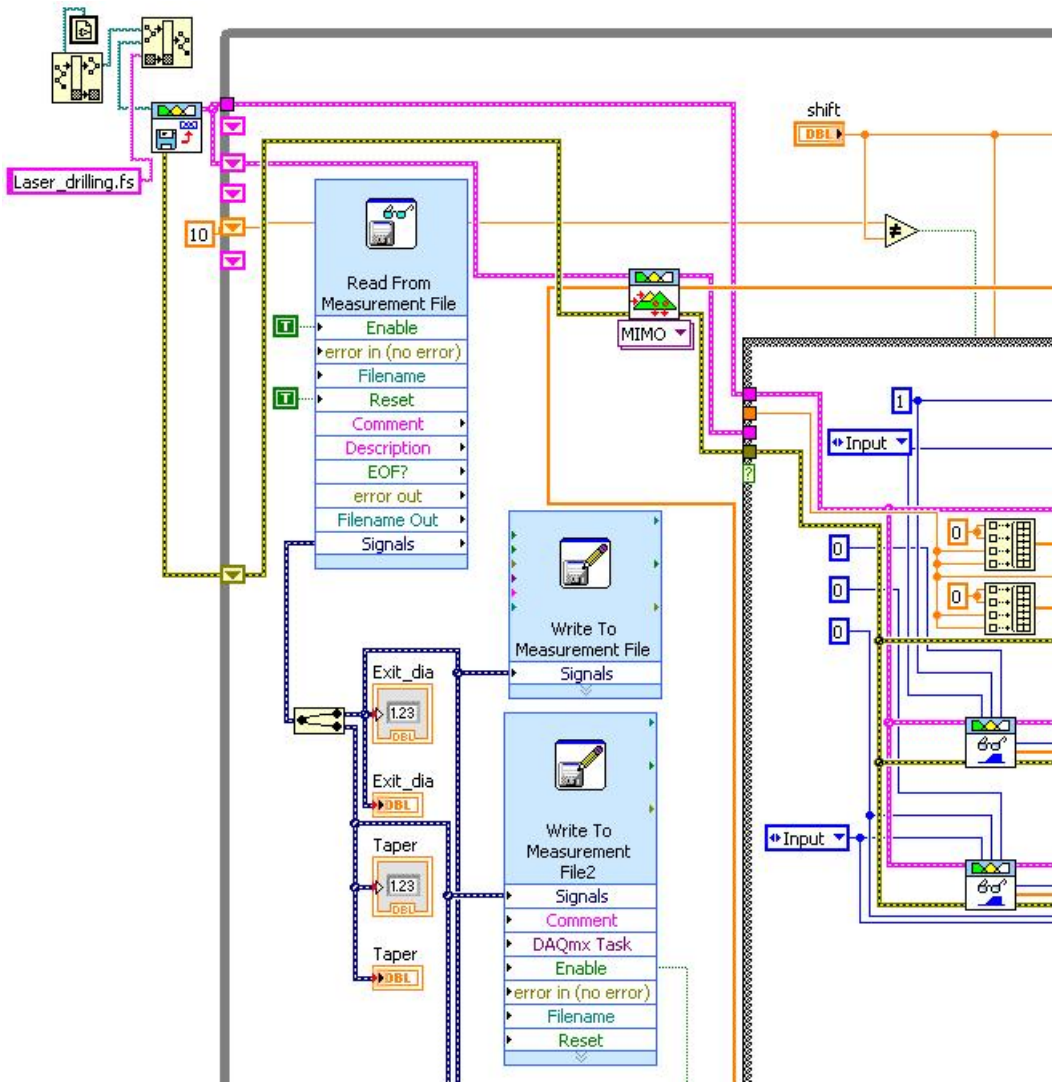


Fig. 6. A section of Fuzzy logic controller on LabVIEW

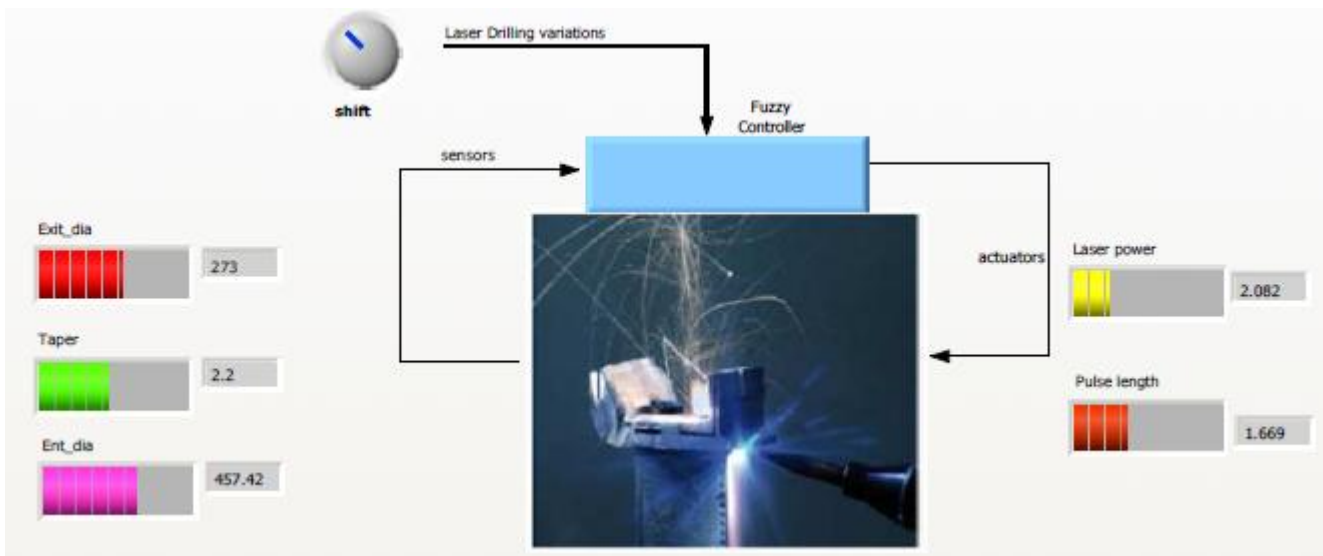


Fig. 7. Fuzzy logic controller front panel

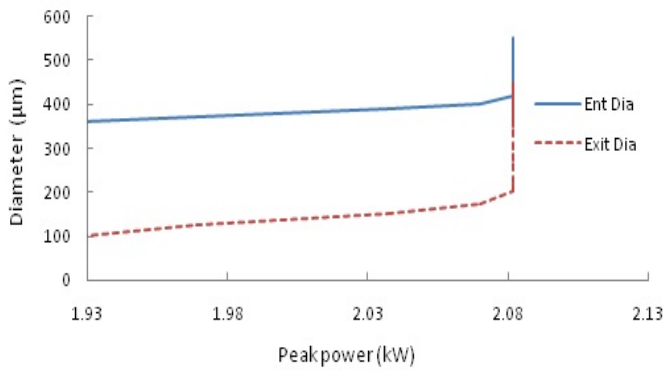


Fig. 8. Effect of laser peak power on hole diameters

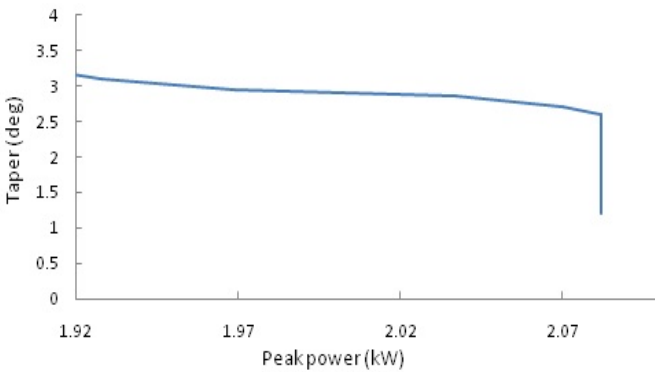


Fig. 9. Effect of laser peak power on hole taper

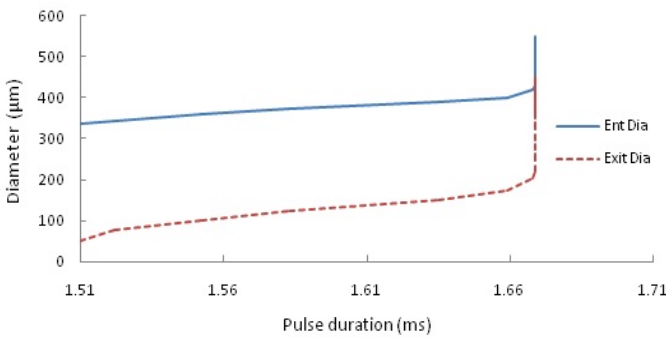


Fig. 10. Effect of laser pulse duration on hole diameters

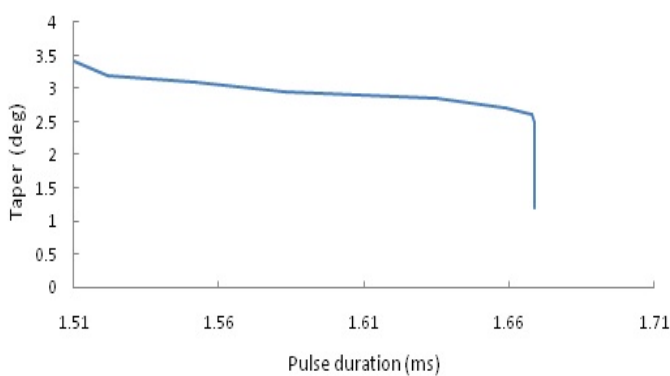


Fig. 11. Effect of laser pulse duration on hole taper

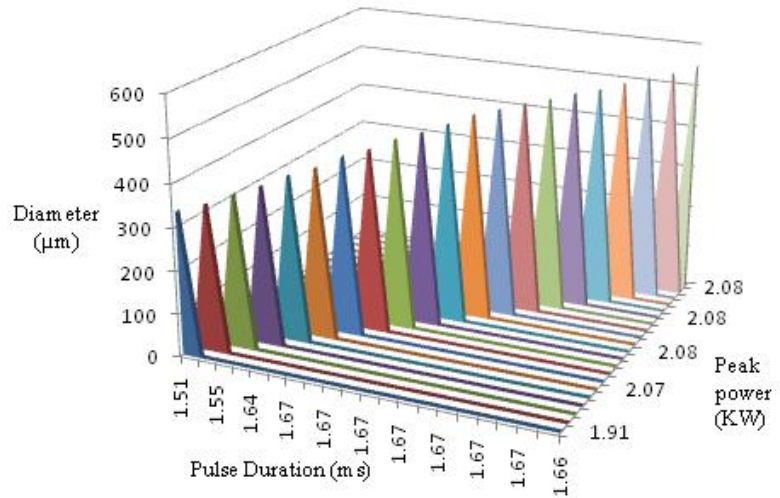


Fig. 12. Surface map for entrance hole diameters

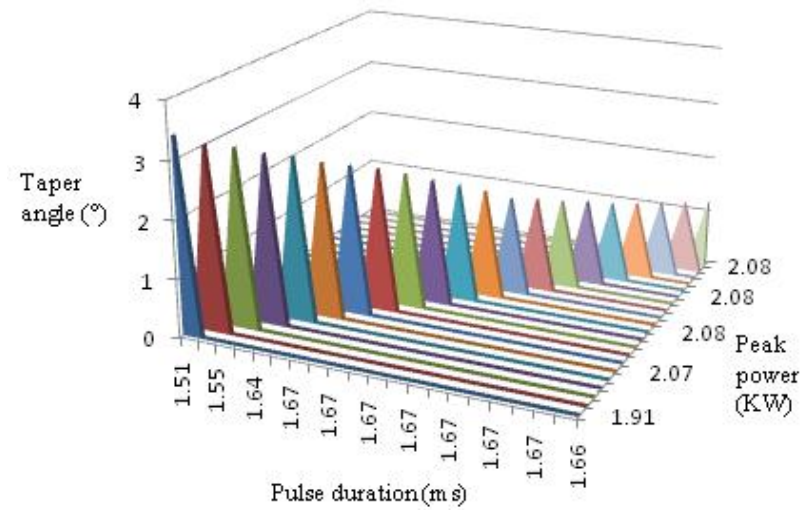


Fig. 13. Surface map for hole taper angles

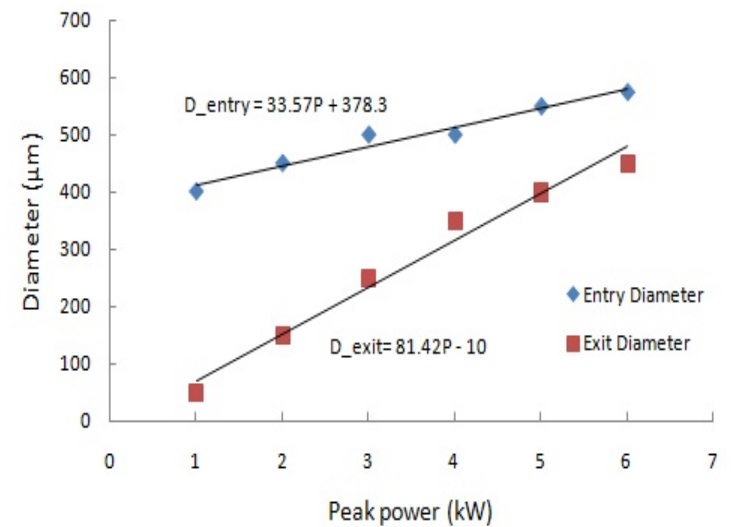


Fig. 14. Rate of change of hole diameters with peak power

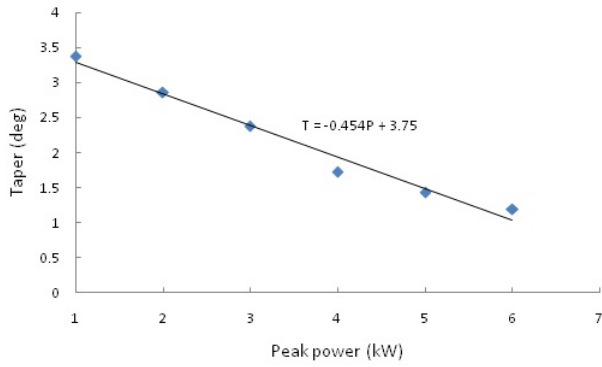


Fig. 15. Rate of change of hole taper with peak power

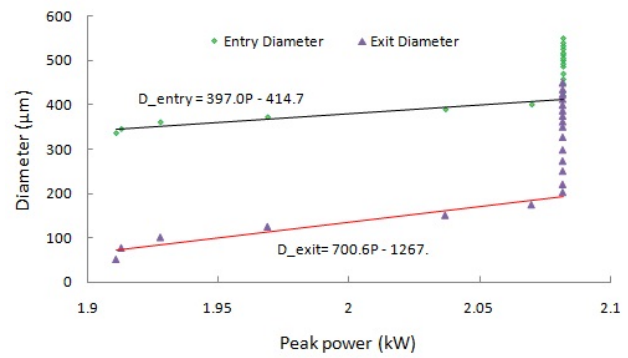


Fig. 18. Rate of change of hole diameters with peak power while using the controller

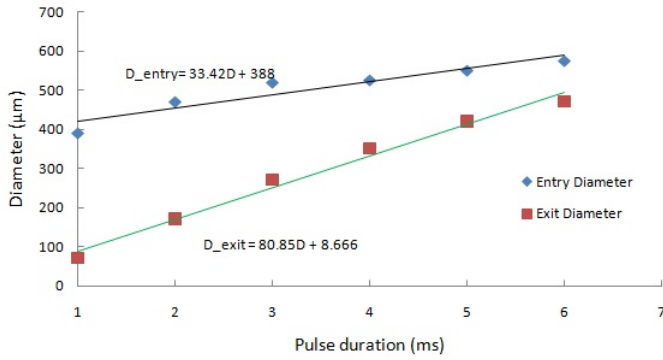


Fig. 16. Rate of change of hole diameters with pulse duration

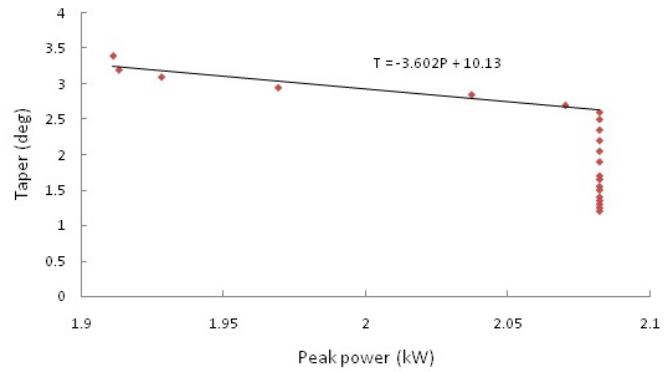


Fig. 19. Rate of change of hole taper with peak power while using the controller

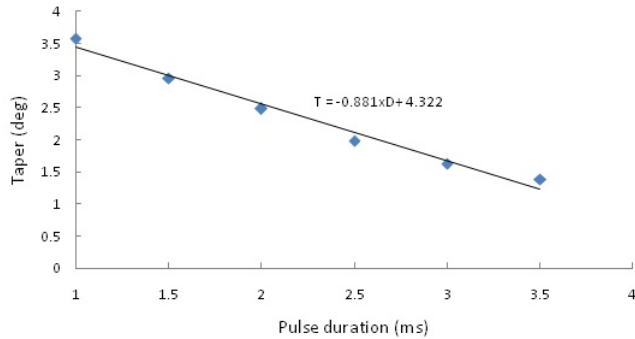


Fig. 17. Rate of change of hole taper with pulse duration

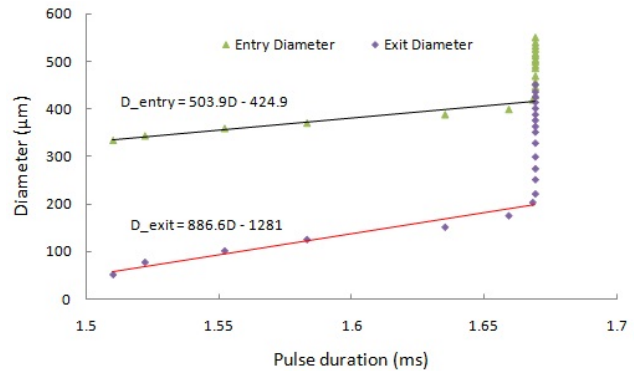


Fig. 20. Rate of change of hole diameters with pulse duration while using the controller

Figures 18 through 21 show the rates of change of hole diameters and taper with increase in peak power and pulse duration. The hole entrance diameters increase at an average rate of 0.4 mm/kW and 0.5 mm/ms while the exit hole diameters increase at an average rate of 0.7 mm/kW and 0.89 mm/ms upto the optimum level of peak power and pulse duration. The hole taper decreases at an average rate of 4.55 deg/kW and 3.6 deg/ms upto the optimum level of peak power and pulse duration.

5. Conclusions

In this paper, a neuro-fuzzy controller for laser percussion drilling was developed. The controller was tested by simulating a laser drilling environment. While drilling without the controller, the hole diameters increase with

increasing laser peak power and pulse duration. Increasing the pulse width at fixed peak power effectively increases energy per pulse of the laser beam. This will generate high vapour pressure built up inside the hole and ejecting more material. Increasing laser peak power at a fixed pulse duration increases the laser beam intensity at the drilling spot.

It was demonstrated that a neuro-fuzzy based controller effectively controls the hole diameters and taper through in-process adjustments of laser power and pulse duration.

While using the controller, the hole diameters increase with increase in peak power and pulse duration upto an

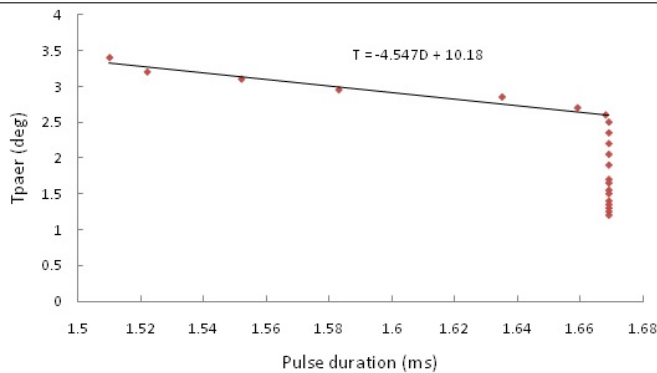


Fig. 21. Rate of change of hole taper with pulse duration while using the controller

optimum level beyond which the peak power and pulse duration remain constant as the diameters increase. The hole taper decreases with increase in peak power and pulse duration upto optimum level beyond which the peak power and pulse duration remain constant as the taper decreases. Thus, the controller helps maintain the peak power and pulse duration at optimum levels.

Acknowledgments

This work has been sponsored by Jomo Kenyatta University of Agriculture and Technology.

References

- [1] Sushant D., Nishant S., Purohit R., *A review on laser drilling and its Techniques*, Proceedings: International Conference on Advances in Mechanical Engineering 2006, AME 2006.
- [2] Roos S.O., *Laser Drilling with Different Pulse Shapes*, Journal of Applied Physics, vol. 51, pp. 5061-5063.
- [3] Steen W.M., *Laser material processing*, Springer-Verlag, London, 1991.
- [4] Prasad G. et al., *Laser cutting of metallic coated sheet steels*, Journal of Materials Processing Technology, vol 74. pp. 234-242, 1998.
- [5] Okasha M.M., Mativenga P.T., Driver N., Li L., *Sequential laser and mechanical micro-drilling of Ni superalloy for aerospace application*, Journal of Manufacturing Technology 59, pp. 199-202, 2010.
- [6] Ravindra H.P., *14. Thermal modeling of laser drilling and cutting of engineering materials*, University of Pune, India, 2005.
- [7] Leigh S., Sezer K., Li L., Grafton-Reed C., Cuttall M., *Recast and oxide formation in laser-drilled acute holes in CMSX-4 nickel single-crystal super-alloy*, Proceedings of the Institution of Mechanical Engineers, Part B: Journal of Engineering Manufacture 224, pp. 1005-1016, 2010.
- [8] Narendra B.D., Sandip P.H., *Laser Fabrication and Machining of Materials*, New York, USA, 2007.
- [9] John F. R., *Industrial applications of lasers*, Academic Press (USA), second edition, 1997.
- [10] Thamir K.I., Rahman M.M., Ahmed N.A., *Improvement of gas turbine performance based on inlet air cooling systems: A technical review*, International Journal of Physical Sciences Vol. 6(4), pp. 620-627, 2011.
- [11] Naeem M., Mike W., *Laser percussion drilling of coated and uncoated aerospace materials with a high beam quality and high peak power lamp pumped pulsed Nd:YAG laser*, Laser Institute of America, ICALEO 2010, pp. 305.
- [12] Ghoreishi M., Low D.K.Y., Li L., *Statistical modelling of laser percussion drilling for hole taper and circularity control*, Proceedings of the Institution of Mechanical Engineers, Part B: Journal of Engineering Manufacture, pp. 307-319, 2002.
- [13] Wei H., *Computational and experimental investigations of laser drilling and welding for microelectronic packaging*, Worcester Polytechnic Institute, 2004.
- [14] Sizov M.A., *Air-film cooling through laser drilled holes*, Eindhoven University of Technology, Netherlands, 2007.
- [15] Patrick H.W., *Artificial Intelligence*, Pearson Education (Singapore), Third Edition, 2004.
- [16] Kurzweil R., *The age of intelligent machines*, MIT Press, Third edition, 1992.
- [17] Witold P., *Fuzzy control and Fuzzy systems*, Research Studies Press Ltd, Second extended edition, 1993.
- [18] Clarence W.S., *Intelligent control, fuzzy logic applications*, CRC press, 1995.
- [19] Fakhreddine O.K., Clarence S., *Soft Computing and Intelligent Systems Design*, Pearson Education (UK), 2004.
- [20] Ali Z., Mohammad J., *Intelligent Control Systems Using Soft Computing Methodologies*, CRC Press, 2001.
- [21] Yang J.R., *ANFIS: Adaptive-Network-Based Fuzzy Inference System*, IEEE Trans. on systems, man, and cybernetic, vol. 23, no.3, pp. 665-685, May 1993.
- [22] Alexander M.M., James S.A., *Intelligent systems, Architecture, Design, and control*, John Wiley & Sons, Inc (New York), 2002.
- [23] Seema C., Mitra R., Kumar V., *A Neuro-fuzzy Learning and its Application to Control system*, World Academy of Science, Engineering and Technology 34, 2007.
- [24] Joonghan Shin., *Measurement and numerical simulation of high temperature laser material processing*, University of Michigan, 2010.
- [25] Satapathy B.B., Rana J., and Maity P.K., *Quality Optimization of Micro-Hole In Laser Drilling*, IOSR Journal of Engineering, Vol.2(3) pp:382-388, Mar. 2012.